

Dislocations in extruded Co-49.3at% Al

D. L. YANEY, A. R. PELTON*, W. D. NIX

Department of Materials Science and Engineering, Stanford University, Stanford, California 94305, USA

**Ames Laboratory, Iowa State University, Ames, Iowa 50011, USA*

Polycrystalline Co-49.3at% Al which had been extruded at 1505 K was examined using transmission electron microscopy. Diffraction contrast analysis showed that $\mathbf{b} = \langle 100 \rangle$ as well as $\mathbf{b} = \langle 111 \rangle$ dislocations contribute to elevated temperature deformation in CoAl. Therefore, it was concluded that sufficient slip systems exist in CoAl to allow for general plasticity in the absence of diffusional mechanisms. Since no examples of $\mathbf{b} = \langle 110 \rangle$ dislocations were found, the importance of $\langle 110 \rangle \{1\bar{1}0\}$ slip in CoAl at 1505 K is unclear. Dislocations of the type $\mathbf{b} = \langle 001 \rangle$ were observed on both $\{110\}$ and $\{100\}$ planes while $\mathbf{b} = \langle 111 \rangle$ dislocations were observed on $\{1\bar{1}0\}$ planes.

1. Introduction

In recent years, the search for a new class of high temperature structural materials has led to a renewed interest in the intermetallic, B2 (CsCl) aluminides. Specifically, the materials of greatest interest have been NiAl and CoAl. Both NiAl and CoAl have extremely high melting points (1913 and 1921 K, respectively), exist over a range of compositions and have the potential for self-protection in oxidizing atmospheres. Despite these similarities however, the creep strength of CoAl is noticeably superior to that of NiAl [1]. In order to understand this difference in strength, it is necessary to examine the slip systems that operate in these materials.

For NiAl, it is generally agreed that $\langle 001 \rangle \{110\}$ is the preferred slip system [2-4]. However, if only $\langle 001 \rangle \{110\}$ slip occurs, five independent slip systems are not present and the condition for general plasticity in the absence of diffusional mechanisms is not met. As a result, a major goal of past research on NiAl has been to provide evidence of the operation of additional slip systems. At temperatures below $0.45 T_m$, where T_m is the melting temperature, Pascoe and Newey [4], using surface slip trace analysis of single crystals, observed $\langle 001 \rangle$ slip on $\{100\}$ and $\{210\}$ type planes as well as $\langle 001 \rangle \{110\}$ slip. However, in single crystals oriented to prevent slip in $\langle 100 \rangle$ type directions, $\langle 111 \rangle$ type slip was reported. Pascoe and Newey noted the operation of the $\langle 111 \rangle \{12\bar{3}\}$ slip system while Loretto and Wasilewski [5] provided evidence for the operation of the $\langle 111 \rangle \{11\bar{2}\}$ and $\langle 111 \rangle \{1\bar{1}0\}$ slip systems.

At temperatures above $0.45 T_m$, $\langle 001 \rangle \{110\}$ and $\langle 001 \rangle \{100\}$ type slip are still observed in NiAl single crystals oriented to allow slip in $\langle 001 \rangle$ directions [6, 7]. However, in crystals oriented so as to prevent $\langle 001 \rangle$ slip, operation of the $\langle 1\bar{1}0 \rangle \{110\}$ [7] and $\langle 111 \rangle \{11\bar{2}\}$ [4] slip systems has been documented. It should be noted at this point that slip in the $\langle 111 \rangle$ direction has been observed in polycrystalline NiAl as well as in single crystals of NiAl oriented to prevent

$\langle 001 \rangle$ slip. Lloyd and Loretto [8] observed dislocations with Burgers vectors of the type $\langle 100 \rangle$, $\langle 110 \rangle$ and $\langle 111 \rangle$ in extruded NiAl. Thus, it is clear that five independent slip systems operate in NiAl. Diffusional mechanisms are not needed to provide general plasticity in this material.

As can be seen from the previous discussion, considerable information exists in the literature concerning slip systems in NiAl. Unfortunately, similar information does not exist for CoAl. Thus, as a first step toward understanding the factors which control elevated temperature deformation in CoAl, transmission electron microscopy (TEM) has been used to identify the slip systems that operate in CoAl.

2. Experimental procedure

A Co-49.3 at % Al alloy with a nominal grain size of $15 \mu\text{m}$ was supplied by the NASA Lewis Research Center in the form of extruded rod (16:1 reduction at 1505 K). Portions of the rod received an additional annealing treatment of 2.5 h at 1400 K after extrusion. An electro-discharge machine was used to prepare 1 mm thick transverse sections from the extruded as well as the extruded and annealed rods. After reducing the thickness of the slabs to approximately $250 \mu\text{m}$ by grinding, an electro-discharge machine was used to cut out 3 mm diameter discs. The 3 mm discs were then thinned electrolytically at room temperature in an 8% perchloric-acetic acid solution. Thinned discs were examined in a Philips EM400 microscope operated at 120 kV.

The character of the dislocations was determined from diffraction contrast experiments. Images were formed from at least twelve different two-beam conditions with s (the vector describing the deviation from the exact Bragg condition) slightly positive in all cases. Residual contrast effects arising from the orientation of dislocations within the foil were taken into account by use of both the $\mathbf{g} \cdot \mathbf{b} = 0$ and $(\mathbf{g} \cdot \mathbf{b}) \times \mathbf{u} = 0$ invisibility criteria. A minimum of two cases of effective invisibility were required for each Burgers vector

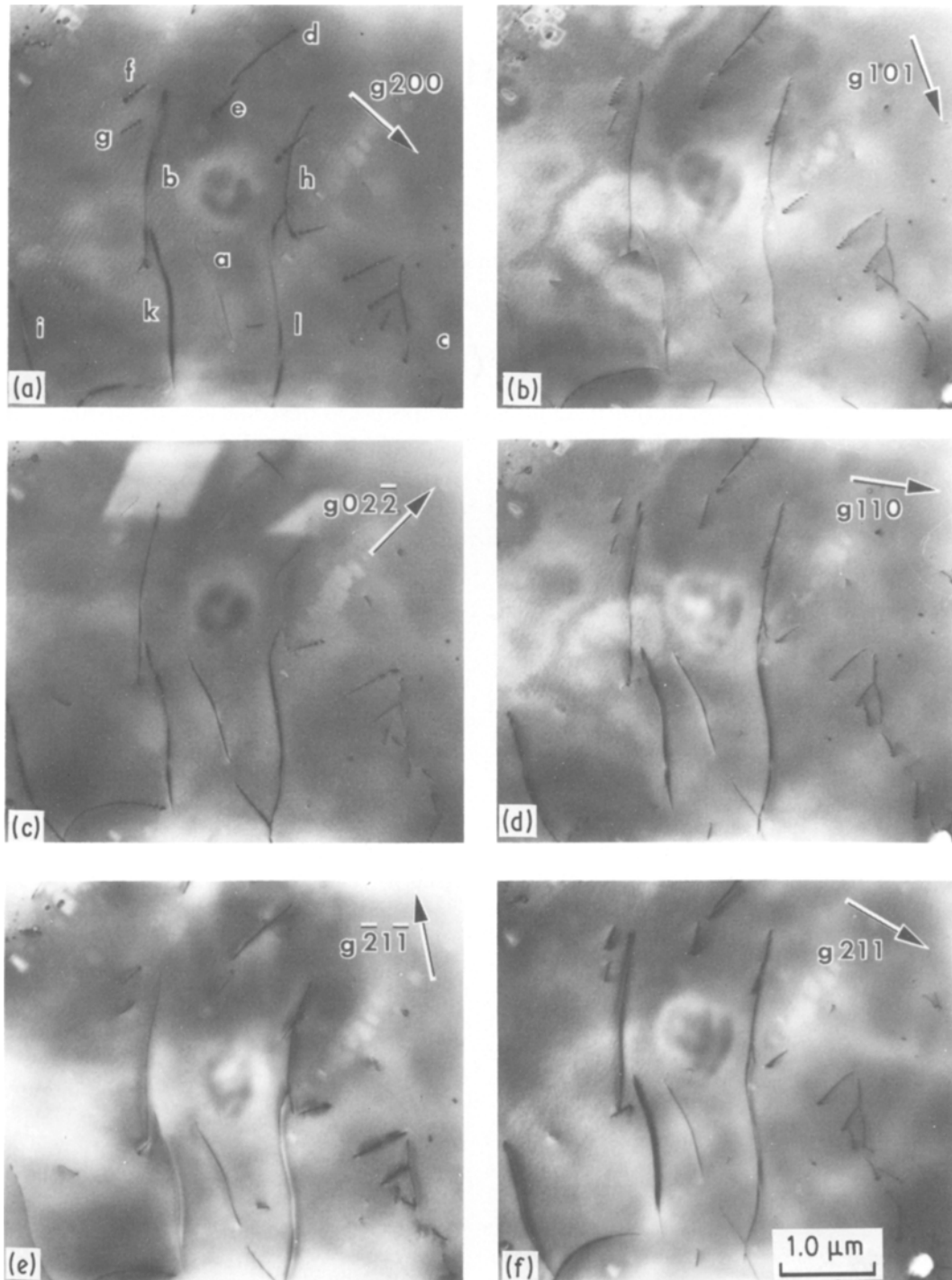


Figure 1 An analysis of Burgers vectors of dislocations in extruded and annealed Co-49.3 at % Al. The electron beam was close to $[011]$ for (a), (c) and (e) and close to $[\bar{1}11]$ for (b), (d) and (f). The diffracting vectors are indicated.

assignment. Dislocation line directions and slip planes were determined by stereographic trace analysis.

3. Results

Fig. 1 shows the results of a diffraction contrast analysis of dislocations in extruded and annealed Co-49.3 at % Al. As in other materials with the B2 crystal structure, dislocations of the type $b = \langle 100 \rangle$ are readily observed in CoAl. For example, dislocation *a* shows only residual contrast with $g\ 200$ and $g\ 101$ and therefore must be of the type $b = [010]$. Similarly, dislocation *b*, as well as the three short dislocations at *c*, exhibit only weak contrast when imaged using $g\ 200$ and $g\ 110$ and therefore must be of the type

$b = [001]$. Dislocations *d-h*, on the other hand, are out of contrast only for $g\ 02\bar{2}$ and thus Burgers vectors $[100]$ and $[111]$ are both possible. However, if in CoAl, as in NiAl, $\langle 100 \rangle$ slip is much easier than $\langle 111 \rangle$ slip, a majority of the unidentified dislocations are likely to have $b = [100]$. Additional $b = \langle 100 \rangle$ type dislocations can be seen to make up the twist boundary shown in Fig. 2. The dislocations visible in Figs 2a and b are screw dislocations with $b = [010]$ while the dislocations visible in Figs 2c and d are screw dislocations with $b = [100]$. Both sets of dislocations lie in the (001) plane.

In addition to $b = \langle 100 \rangle$ type dislocations, $b = \langle 111 \rangle$ type dislocations are also present in the

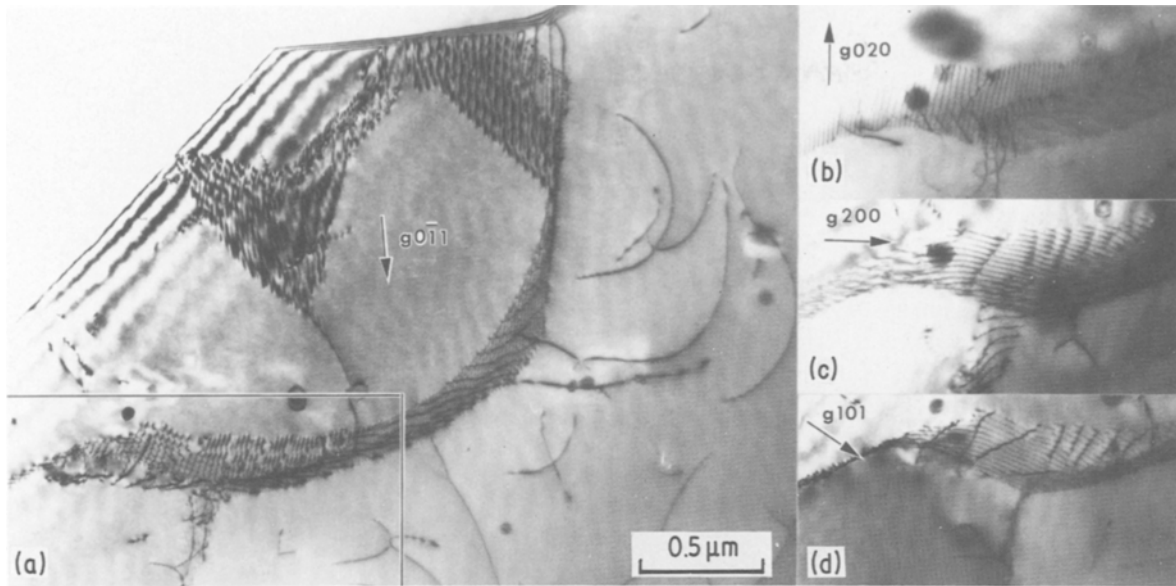


Figure 2 Twist boundary in extruded Co-49.3 at % Al. The electron beam was close to $[011]$ in (a), close to $[001]$ in (b) and (d) and close to $[\bar{1}11]$ in (d). The diffracting vectors are indicated.

extruded and annealed CoAl. Dislocations i , k and l in Fig. 1 are all edge dislocations with $\mathbf{b} = [11\bar{1}]$. They lie along the $[\bar{2}1\bar{1}]$ direction in the (011) plane and exhibit only residual contrast for $\mathbf{g}\bar{2}1\bar{1}$ and $\mathbf{g}101$. It should be noted that complete invisibility is not expected for edge dislocations unless both $\mathbf{g} \cdot \mathbf{b} = 0$ and $(\mathbf{g} \cdot \mathbf{b}) \times \mathbf{u} = 0$. For $\mathbf{g}101$, $(\mathbf{g} \cdot \mathbf{b}) \times \mathbf{u} = 1.22$ and complete invisibility is not expected for dislocations i , k and l . However, for $\mathbf{g}\bar{2}1\bar{1}$, the vector products $\mathbf{g} \cdot \mathbf{b}$ and $(\mathbf{g} \cdot \mathbf{b}) \times \mathbf{u}$ are both zero and thus complete invisibility is expected. The fact that residual contrast is observed for $\mathbf{g}\bar{2}1\bar{1}$ indicates that CoAl is anisotropic. This is not unreasonable in view of the fact that NiAl containing 49.3 at % Al has an anisotropy factor, A , of 3.3 at room temperature [9] and exhibits image characteristics similar to those of CoAl. At the same time however, it should be noted that Co-49.3 at % Al is probably not as anisotropic as the B2 compound β -CuZn ($A = 7.8$) where strong contrast is observed even when both $\mathbf{g} \cdot \mathbf{b}$ and $(\mathbf{g} \cdot \mathbf{b}) \times \mathbf{u} = 0$ [10].

4. Discussion

4.1. Slip systems

As noted in the previous section, several examples of $\mathbf{b} = \langle 100 \rangle$ and $\mathbf{b} = \langle 111 \rangle$ type dislocations were observed in CoAl. Many of these dislocations were long and only slightly curved suggesting that both $\mathbf{b} = \langle 100 \rangle$ and $\mathbf{b} = \langle 111 \rangle$ dislocations contribute to elevated temperature deformation in CoAl. Therefore, sufficient slip systems apparently exist in CoAl to allow for general deformation without the assistance of diffusional mechanisms.

In an investigation of extruded NiAl, Lloyd and Loretto [8] concluded that $\mathbf{b} = \langle 110 \rangle$ as well as $\mathbf{b} = \langle 100 \rangle$ and $\mathbf{b} = \langle 111 \rangle$ dislocations contribute to elevated temperature deformation in NiAl. However, since no examples of $\mathbf{b} = \langle 110 \rangle$ dislocations were found in this investigation, the importance of $\langle 110 \rangle \{1\bar{1}0\}$ slip in CoAl during extrusion at 1505 K is in doubt.

Although results of the present investigation indicate that sufficient slip systems are present in CoAl for general deformation at elevated temperatures, it is important to realize that the stress required to produce slip may vary considerably from slip system to slip system. For example, in NiAl, both $\langle 100 \rangle$ and $\langle 111 \rangle$ slip have been observed at temperatures as low as 77 K [4, 5]. However, as noted by Ball and Smallman [11], NiAl single crystals oriented to prevent $\langle 100 \rangle$ slip (compression axis parallel to $\langle 100 \rangle$) are 20 times stronger than crystals oriented to allow $\langle 100 \rangle$ slip (compression axis parallel to $\langle 110 \rangle$) even at temperatures of 823 K. Thus it seems probable that in CoAl, $\langle 100 \rangle$ slip is much easier than $\langle 111 \rangle$ slip.

Unlike $\langle 100 \rangle$ and $\langle 111 \rangle$ slip, $\langle 110 \rangle$ slip has been observed to contribute to deformation in NiAl only at temperatures above approximately 750 K. Furthermore, Bevk *et al.* [7] noted that the amount of $\langle 110 \rangle$ slip increases with increasing temperature. Thus, based on experimental evidence it appears that $\langle 110 \rangle$ slip is more difficult than either $\langle 100 \rangle$ or $\langle 111 \rangle$ slip.

Previously, Ball and Smallman [2] estimated the relative mobility parameter, S of the various dislocations in NiAl using the equation proposed by Eshelby [12],

$$S = \left(\frac{4\pi\delta}{b} \right) \exp \left(- \frac{2\pi\delta}{b} \right) \quad (1)$$

where δ is the width of the dislocation and a low value of S corresponds to a high mobility. Based on their calculations, $\mathbf{b} = \langle 110 \rangle$ dislocations should glide easily on $\{1\bar{1}0\}$ planes in direct contrast to experimental evidence. However, as pointed out by Potter [13], the relative mobility parameter, S , is often not an accurate guide to the ease of dislocation motion in B2 compounds. The parameter S can be defined as the ratio of the stress needed to move a dislocation in its slip plane to the stress required to rigidly slip an entire plane of atoms over an adjacent plane. Hence, S depends primarily on elastic constants which in turn are an accurate representation of material behaviour

only when atoms are in their equilibrium lattice positions. Thus, for B2 compounds such as NiAl where the resistance to $\langle 110 \rangle \{1\bar{1}0\}$ shear is quite small [9], a low resistance to $\langle 110 \rangle \{1\bar{1}0\}$ glide of dislocations is incorrectly predicted by the relative mobility parameter. It must be remembered that for the movement of a $\langle 110 \rangle$ dislocation on a $\{1\bar{1}0\}$ plane to proceed, like atoms must pass directly over one another at a distance of closest approach of $0.707a$. In strongly ordered compounds such as NiAl or CoAl where bonding between unlike atoms is preferred, movement of $\langle 110 \rangle \{1\bar{1}0\}$ dislocations is expected to be quite difficult. From this point of view, it is not surprising that no examples of $b = \langle 110 \rangle$ dislocations were observed in CoAl even after extrusion at 1505 K. Apparently in CoAl, as in NiAl, activation of the $\langle 110 \rangle \{1\bar{1}0\}$ slip system is difficult.

4.2. Directional instability of dislocations

In 1967, Head [14] showed that the energy of a dislocation in an anisotropic crystal depends on the crystallographic direction of the dislocation line. A straight dislocation in a high energy direction may become zigzagged even though this would result in an increase in line length. This effect could be of importance in explaining the high temperature strength of the crystal.

In the present investigation, no zigzagged dislocations were observed in CoAl even though this material is suspected to be fairly anisotropic ($A \approx 3$). Furthermore, since examples of zigzagged dislocations have been clearly noted in other B2 compounds [5, 15], it was desirable to determine whether or not the dislocations observed in CoAl were in high energy orientations where zigzagged shapes should be expected.

The easiest way to determine unstable orientations is to construct an inverse Wulff plot. In this type of plot, the inverse of the line energy [16] of a dislocation is plotted in polar coordinates as a function of the angle between the Burgers vector and the dislocation line. A schematic inverse Wulff plot is shown in Fig. 3a. If the curve were everywhere convex, the dislocation would be stable in all orientations. However, in the schematic plot of Fig. 3a, concavities exist, indicating that the dislocation is unstable for certain orientations. Specifically, according to the DeWit and Koehler criterion, the dislocation is unstable for orientations between the inflection points A and B and between the inflection points C and D.

Actual construction of an inverse Wulff plot requires knowledge of material elastic constants. Since elastic constant data are not available for CoAl, inverse Wulff plots were constructed using the elastic constants for Ni-49.3 at % Al at 623 K, the highest temperature for which data are available [9]. Inverse Wulff plots for the $\langle 1\bar{1}1 \rangle \{011\}$, $\langle 0\bar{1}1 \rangle \{011\}$, $\langle 100 \rangle \{011\}$ and $\langle 100 \rangle \{001\}$ slip systems are shown in Figs 3b to e respectively. In these plots, 0° corresponds to a pure screw orientation while 90° corresponds to a pure edge orientation. As can be seen in Fig. 3b, $b = \langle 1\bar{1}1 \rangle$ dislocations should be unstable only for a small range of orientations about 45° and 225° . Thus, it is not surprising that the $b = \langle 1\bar{1}1 \rangle$ edge dislocations seen in Fig. 1 are not sharply bent. The Wulff plot in

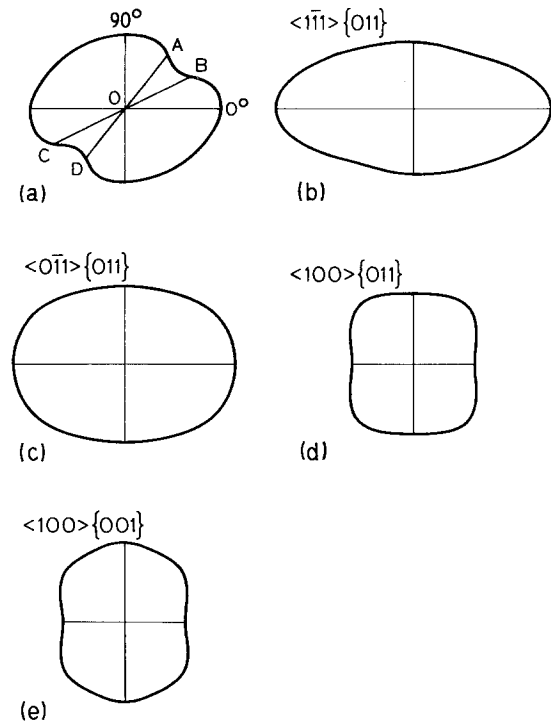


Figure 3 (a) Schematic inverse Wulff plot. Dislocation is unstable for any direction between OA and OB and between OC and OD. Inverse Wulff plots for the (b) $\langle 1\bar{1}1 \rangle \{011\}$, (c) $\langle 0\bar{1}1 \rangle \{011\}$, (d) $\langle 100 \rangle \{011\}$ and (e) $\langle 100 \rangle \{001\}$ slip systems in CoAl. Elastic constants used are those for Ni-49.3 at % Al at 623 K [9].

Fig. 3c shows that $\langle 0\bar{1}1 \rangle$ dislocations on $\{011\}$ planes should be stable in all orientations. From Fig. 3d it is apparent that $b = \langle 100 \rangle$ dislocations on $\{011\}$ planes are unstable about both pure screw and pure edge orientations. Dislocations of the type $b = \langle 100 \rangle$ on $\{001\}$ planes, on the other hand, can be seen in Fig. 3e to be unstable only about the screw orientation. In agreement with the above predictions, none of the $b = \langle 100 \rangle$ dislocations in Fig. 1, all of which are of mixed character, exhibit the sharp bends characteristic of dislocations in high energy orientations. The $b = \langle 100 \rangle$ type dislocations making up the twist boundary shown in Fig. 2, however, are of screw orientation and hence would be expected to be zigzagged. The fact that these $b = \langle 100 \rangle$ dislocations appear fairly straight may have a number of explanations. First of all, it is possible that the zigzag pattern is so fine that it is not visible in Fig. 2. Secondly, stresses from the many other parallel dislocations in the boundary may cause the higher energy screw orientation to be maintained. Finally, it is possible that the use of NiAl elastic constants instead of CoAl elastic constants results in an incorrect inverse Wulff plot construction. It should be noted that the twist boundary seen in Fig. 2 was examined using several different beam directions. This eliminated the possibility that a zigzag was not visible in a particular instance because the dislocation was bent in a plane perpendicular to the projection plane.

Except for the screw dislocations within the twist boundary of Fig. 2, the inverse Wulff plot construction predicts that all the dislocations identified in this investigation lie in stable orientations. Therefore it is not surprising that no sharply bent dislocations were

observed. However, sharply bent dislocations might be observed in CoAl if a large number of dislocations were examined.

Acknowledgements

This work was sponsored by the NASA Lewis Research Center under Grant No. NASA NAG 3-248. The authors thank Dr J. D. Whittenberger of the NASA Lewis Research Center for initiating this project and for providing the material for this study. The assistance of Professor D. M. Barnett of Stanford University in constructing the inverse Wulff plots is gratefully acknowledged.

References

1. L. A. HOCKING, P. R. STRUTT and R. A. DODD, *J. Inst. Met.* **99** (1971) 98.
2. A. BALL and R. E. SMALLMAN, *Acta Met.* **14** (1966) 1517.
3. R. J. WASILEWSKI, S. R. BUTLER and J. E. HANLON, *Trans. AIME* **239** (1967) 1357.
4. R. T. PASCOE and C. W. A. NEWBY, *Phys. Status Solidi* **29** (1968) 357.
5. M. H. LORETTO and R. J. WASILIEWSKI, *Phil. Mag.* **23** (1971) 1311.
6. P. R. STRUTT, R. A. DODD and G. M. ROWE, in Proceedings of the Second International Conference on the Strength of Metals and Alloys, Pacific Grove, August 1970 (ASM, Metals Park, Ohio, 1970) p. 1057.
7. J. BEVK, R. A. DODD and P. R. STRUTT, *Metall. Trans.* **4** (1973) 159.
8. C. H. LLOYD and M. H. LORETTO, *Phys. Status Solidi* **39** (1970) 163.
9. N. RUSOVIC and H. WARLIMONT, *ibid.* **44** (1977) 609.
10. P. HUMBLE, in "Diffraction and Imaging Techniques in Material Science", Vol. I. edited by S. Amelickx, R. Gevers and J. Van Landuyt (North-Holland, New York, 1978) p. 315.
11. A. BALL and R. E. SMALLMAN, *Acta Met.* **14** (1966) 1349.
12. J. D. ESHELBY, *Phil. Mag.* **40** (1949) 903.
13. D. I. POTTER, *Mater. Sci. Eng.* **5** (1969/70) 208.
14. A. K. HEAD, *Phys. Status Solidi* **19** (1967) 185.
15. H. SAKA, *Phil. Mag.* **49** (1984) 327.
16. D. M. BARNETT, R. J. ASARO, S. D. GAVAZZA, D. J. BACON and R. O. SCATTERGOOD, *J. Phys. F: Met. Phys.* **2** (1972) 854.

*Received 3 July
and accepted 8 August 1985*